PERGAMON

International Journal of Solids and Structures 37 (2000) 4403–4417

INTERNATIONAL JOURNAL OF SOLIDS and STRUCTURES

www.elsevier.com/locate/ijsolstr

Dynamics of elastic-piezoelectric two-layer beams using spectral element method

Usik Lee*, Joohong Kim

Department of Mechanical Engineering, Inha University, 253 Yonghyun-Dong, Nam-Ku, Inchon, 402-751, South Korea

Received 22 October 1998; in revised form 6 May 1999

Abstract

It is important to predict the dynamic characteristics of a piezoelectrically actuated beam very accurately for successful vibration controls. It has been well recognized that spectral elements provide very accurate solutions for such simple structures as beams. Thus, this paper introduces a spectral element method (SEM) and a spectral-element based modal analysis method (MAM) for elastic-piezoelectric two-layer beams. The axial-bending coupled equations of motion are derived first by using Hamilton's principle and the spectral element matrix is formulated from the spectrally formulated exact eigenfunctions of the coupled governing equations. For MAM, the orthogonality of the eigenfunctions (i.e. natural modes) is proved. Present solution approaches are verified by comparing their results with the conventional FEM results. It is shown that the results by MAM and FEM converge to those by SEM as the number of superposed natural modes and the number of discretized finite elements are increased, respectively. It is also shown that, as the thickness of piezoelectric layer vanishes, the axial-bending coupled problems are decoupled to yield the solutions for two independent problems: the pure axial-motion problem and the pure bending-motion problem.

Keywords: Special element method; Modal analysis; Two-layer beam; Piezoelectric actuator; Coupled equations of motion

1. Introduction

Piezoelectric materials have received considerable attention due to their potential applications to the active controls of structural vibration and noise. The converse piezoelectric effect is used for the actuator design while the direct piezoelectric effect is used for the sensor design. In order to use the piezoelectric effects, the piezoelectric materials are usually bonded on the surface of a structure. Thus, the structure becomes a multi-layer laminate structure. Though there should be diverse types of multi-

* Corresponding author. Tel.: +82-32-860-7318; fax: +82-32-866-1434.
E-mail address: ulee@dragon.inha.ac.kr (U. Lee).

0020-7683/00/$ - see front matter
PII: S0020-7683(99)00154-7

layer structure, the discussion in this paper will be confined to the two-layer beam that consists of an elastic base layer and a piezoelectric layer.

It is important to use a satisfactory structure model together with a proper solution method to obtain reliable dynamic characteristics of a multi-layer beam. Historically, there have been developed many analytical structure models for the elastic–elastic two-layer beams (Hess, 1969), the elastic–viscoelastic two-layer beams (Oberst, 1952), the elastic–viscoelastic–elastic three-layer beams (Kerwin, 1959; Mead and Markus, 1969; Yan and Dowell, 1972; Rao and Nakra, 1974; Mead, 1982; Bai and Sun, 1993; Nayfeh and Solocum 1997), the elastic–piezoelectric two-layer beams (Crawley and de Luis, 1987; Shi and Atluri, 1990), and for the elastic–viscoelastic–piezoelastic three-layer beams (Baz, 1993; Liao, 1997). Despite of numerous analytical structure models for multi-layered beams, some models are inappropriate for practical applications. This is in part due to the strict assumptions and in part due to the mathematical complexity used for analytical models. Thus, there also have been developed many finite element models (Robbins and Reddy, 1991; Lesieutre and Lee, 1996). The finite element approach may provide models that are more realistic by removing some strict assumptions that are inevitable for analytical models. However, as a drawback of the finite element method (FEM), extremely precise finite elements discretization is required to obtain reliable dynamic solutions, especially at high frequency. Furthermore, the modal analysis commonly used in conjunction with FEM is limited to the frequency regimes where the relative spacing of natural frequencies remains large compared to the relative parameter uncertainty. Thus, alternatives to FEM have been considered by many researchers.

In the literature, Doyle (1988) used the spectrally formulated finite element, called as the spectral element, to study the wave propagation in structures. In contrast to the conventional finite element, the spectral element treats the mass distribution within a structural element exactly by using exact shape functions and thus it provides accurate dynamic characteristics of a structure. The spectral element matrix is the same as the *exact* dynamic stiffness matrix in nature (Leung, 1993; Banerjee, 1997). In spectral element method (SEM), a structure can be discretized into many spectral elements and the spectral elements can be assembled in a completely analogous way to that used for FEM. The significant difference from FEM is that FFT and inverse FFT algorithms are utilized in SEM. This procedure is known to provide very accurate solutions even at high frequency (Lee and Lee, 1997). Despite the outstanding features of SEM, there have been very few applications to multi-layer structures. This is probably due to the difficulty in obtaining the exact shape functions for such complex structures. In the literature, Leung and Zhou (1996) derived the dynamic stiffness matrix for the laminated composite plate based on an effective single-layer plate model.

The dynamics of a multi-layer structure is usually represented by a set of coupled equations of motion. Diverse coupled structural dynamics problems have been studied by many researchers (Dokumaci, 1987; Bishop et al., 1989; Banerjee, 1989; Banerjee et al., 1996). However, probably due to the mathematical complexity, the modal analysis method (MAM) has not been well applied to such coupled problems in the literature. There are several types of structural coupling. For instance, there are the stiffness coupling of Timoshenko's beam model, the inertia coupling of the bending-torsion coupled vibration problem considered by Dokumaci (1987), and the stiffness and inertia coupling of the multi-layer beams considered in this paper. In the case of Timoshenko's beam problem, the original two coupled dynamic equations can be combined to reduce a single higher order equation of motion so that the modal analysis approach can be readily applied to the problem. However, for the other two coupling problems, the situation is not so simple so a special effort is required to conduct the modal analysis.

It may be important to predict the dynamic characteristics of a piezoelectrically actuated beam accurately for successful vibration and noise control applications. As discussed just before, it has been well known that spectral elements provide very accurate solutions for such simple structures as beams. Thus, the purpose of this paper is to introduce a SEM and a spectral-element based MAM for the

elastic–piezoelectric two-layer beam in which the piezoelectric layer is used an actuator. Thus, in this paper, the spectral element is first formulated from the axial-bending coupled equations of motion for an elastic–piezoelectric two-layer beam. Then, a modal analysis approach for the present axial-bending coupled vibration problem is introduced by deriving the orthogonality property of the natural modes. Finally, the accuracy of the solutions obtained by SEM and MAM is verified.

2. Formulation of the coupled equations of motion

The geometry and deformation of an elastic-piezoelectric two-layer beam of length L is shown in Fig. 1. The structural dynamic equations of motion are derived based on the following assumptions:

1. The shear deformations in both layers are negligible.
2. The rotary inertia is negligible.
3. The transverse displacement $w(x, t)$ is same for both layers.
4. There is perfect continuity, but no slip, at the interface.
5. Liner theories of elasticity and piezoelectricity are applicable.
6. The density and thickness are uniform over the beam.
7. The applied voltage is uniform along the beam.

In Fig. 1, u_b and u_p are the axial displacements of the neutral axes of the base beam and the piezoelectric layer, respectively. For perfect bonding conditions, the geometry of Fig. 1 provides the kinematics relation as

$$u_p = u_b - \frac{h_b + h_p}{2}\theta \tag{1}$$

where h_b and h_p are the thickness of base beam and the thickness of piezoelectric layer, respectively, and $\theta = \partial w/\partial x$ is the rotational angle of the base beam. As used in Eq. (1), the subscripts b and p are used in the following formulations to represent the quantities for the *base* beam layer and *piezoelectric* layer, respectively.

The constitutive equation of the piezoelectric materials under uni-axial loading can be written as

$$\begin{Bmatrix} \sigma \\ E \end{Bmatrix} = \begin{bmatrix} C_{11}^{D} & -h_{31} \\ -h_{31} & \beta_{33}^{s} \end{bmatrix} \begin{Bmatrix} \epsilon \\ D \end{Bmatrix} \tag{2}$$

where σ and ϵ are the mechanical stress and strain in the x-direction, respectively. D is the electrical displacement (charge/area in the beam vertical direction) and E is the electrical field (voltage/length

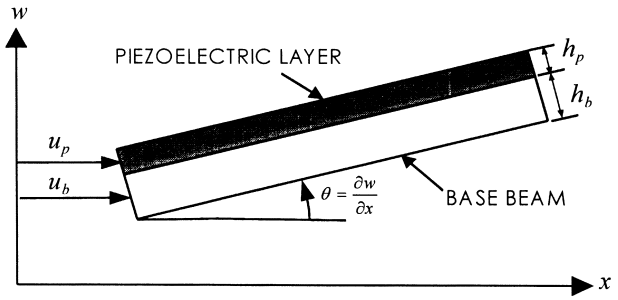

Fig. 1. Geometry and deformation of the elastic-piezoelectric two-layer beam.

along the vertical direction). C_{11}^{D} is the elastic stiffness, β_{33}^{S} is the dielectric constant, and h_{31} is the piezoelectric constant.

Using the above constitutive relation and assuming D is constant through the thickness of thin piezoelectric layer, the strain energy of the two-layer beam is derived after integrating over z and assuming $\epsilon = zw''$ as

$$V = \frac{1}{2}\int_0^L (E_b A_b u_b'^2 + E_b I_b W''^2 + C_{11}^{D} A_p u_p'^2 + C_{11}^{D} I_p w''^2 - 2A_p h_{31} D u_p' + A_p \beta_{33}^{S} D^2)\, dx \tag{3}$$

where E, A, I and ρ (for each layer) are the Young's modulus, the cross-sectional area, the area moment of inertia about the neutral axis, and the mass density, respectively. The kinetic energy of the two-layer beam is also derived as

$$T = \frac{1}{2}\int_0^L \{\rho_b A_b(\dot{u}_b^2 + \dot{w}^2) + \rho_p A_p(\dot{u}_p^2 + \dot{w}^2)\}\, dx. \tag{4}$$

The virtual work is given by

$$\delta W = \int_0^L bV(t)\delta D\, dx + \bar{N}\delta u_b\,|_L^0 + \bar{M}\delta\theta\,|_L^0 + \bar{Q}\delta w\,|_L^0 \tag{5}$$

In the preceding equations, the prime ($'$) and the dot ($\cdot$) indicate the partial derivatives with respect to the coordinate x and the time t, respectively. $V(t)$ is the applied voltage.

The axial displacement of piezoelectric layer u_p can be eliminated from two energy expressions, Eqs. (3) and (4), by using Eq. (1). Applying these energies into Hamilton's principle yields the axial-bending coupled equations of motion as

$$EIw'''' + \rho A\ddot{w} = -\alpha\ddot{u}_b' + \beta u_b''' + \gamma\ddot{w}''$$

$$EAu_b'' - \rho A\ddot{u}_b = -\alpha\ddot{w}' + \beta w''' \tag{6}$$

where

$$\rho A = \rho_b A_b + \rho_p A_p, \quad EA = E_b A_b + E_p A_p, \quad EI = E_b I_b + C_{11}^{D} I_p + \frac{1}{4}E_p A_p h^2$$

$$\alpha = \frac{1}{2}\rho_p A_p h, \quad \beta = \frac{1}{2}E_p A_p h, \quad \gamma = \frac{1}{4}\rho_p A_p h^2$$

$$h = h_b + h_p, \quad E_p = C_{11}^{D} - \frac{h_{31}^2}{\beta_{33}^{S}}. \tag{7}$$

In Eq. (6), α and β are the parameters that govern the axial-bending coupling. Without the piezoelectric constraining layer, the parameters α, β, and γ will vanish to result in two independent de-coupled equations of motion for the pure-bending motion and the pure axial-motion of the base beam.

The Hamilton principle also provides the boundary conditions as

$$N = \bar{N} \quad \text{or} \quad u_b = \bar{u}_b$$

$$M = \bar{M} \quad \text{or} \quad \theta = \bar{\theta}$$

$$Q = \bar{Q} \quad \text{or} \quad w = \bar{w}. \tag{8}$$

The over-bar in Eq. (8) indicates the quantities specified at boundaries. N, M, and Q are the resultant axial force, resultant bending moment, and the resultant transverse shear force Q, respectively. They are related to the mechanical and piezoelectric variables as

$$N = EAu_{\mathrm{b}}' - \beta w'' - bd_{31}E_{\mathrm{p}}V(t)$$

$$M = EIw'' - \beta u_{\mathrm{b}}' + \frac{1}{2}hbd_{31}E_{\mathrm{p}}V(t)$$

$$Q = -EIw''' - \alpha\ddot{u}_{\mathrm{b}} + \beta u_{\mathrm{b}}'' - \gamma\ddot{w}' \tag{9}$$

where d_{31} is the piezoelectric constant defined by $d_{31} = \mathrm{h}_{31}/(E_{\mathrm{p}}\beta_{33}^{\mathrm{S}})$.

The governing equations of motion for the elastic–elastic two-layer beam can be readily reduced from the above formulations by simply eliminating all piezoelectric terms. A similar formulation was given by Liao (1997), but his work was for the cantilevered beam that is *partially* laminated with a piezoelectric patch.

3. Spectral element analysis

The spectral element will be formulated from the general solutions of Eq. (6). Assume that the dynamic responses of beam and the applied voltage have the spectral representations as

$$w(x, t) = \sum_{n}^{N} \hat{W}(x, \omega_n)e^{i\omega_n t}$$

$$u_{\mathrm{b}}(x, t) = \sum_{n}^{N} \hat{U}(x, \omega_n)e^{i\omega_n t}$$

$$V(t) = \sum_{n}^{N} \hat{V}(\omega_n)e^{i\omega_n t} \tag{10}$$

where ω_n is the frequency and $\hat{W}$, $\hat{U}$ and $\hat{V}$ are the spectral components of w, u_{b}, and V, respectively. N is the total number of spectral components summed in Eq. (10). Once the Nyquist frequency ω_{NF} (i.e. the maximum frequency range to be considered in the spectral analysis) is chosen, N is determined by $\omega_{\mathrm{NF}}/\Delta\omega$. Frequency increment $\Delta\omega$ is directly related to the resolution in frequency domain. For shorthand, the summation and subscripts used in Eq. (10) will be omitted in the following.

Substituting Eq. (10) into Eq. (6) and canceling the common time factor may yield coupled two ordinary differential equations for $\hat{W}$ and $\hat{U}$ as

$$EI\hat{W}'''' - \omega^2\rho A\hat{W} = \omega^2(-\gamma\hat{W}'' + \alpha\hat{U}') + \beta\hat{U}'''$$

$$EA\hat{U}'' + \omega^2 \rho A \hat{U} = \omega^2 \alpha \hat{W}' + \beta \hat{W}''''. \tag{11}$$

The general solutions for $\hat{W}$ and $\hat{U}$ can be obtained in the forms of

$$\hat{W}(x) = \sum_{i=1}^{3} (A_i e^{k_i x/L} + A_{2i} e^{-k_i x/L}) = [\mathbf{N}(x)]\{\mathbf{A}\}$$

$$\hat{U}(x) = \sum_{i=1}^{3} (B_i e^{k_i x/L} + B_{2i} e^{-k_i x/L}) = [\mathbf{N}(x)]\{\mathbf{B}\} \tag{12}$$

where

$$[\mathbf{N}(x)] = [\, e^{k_1 x/L}\ e^{k_2 x/L}\ e^{k_3 x/L}\ e^{-k_1 x/L}\ e^{-k_2 x/L}\ e^{-k_3 x/L}]$$

$$\{\mathbf{A}\} = \{A_1\ A_2\ A_3\ A_4\ A_5\ A_6\}$$

$$\{\mathbf{B}\} = \{B_1\ B_2\ B_3\ B_4\ B_5\ B_6\}. \tag{13}$$

In Eq. (12), k_i ($i = 1, 2, 3$) are the wave numbers to be computed from

$$(\beta^2 - EAEI)k^6 + \omega^2 L^2 (2\alpha\beta - \rho AEI - \gamma EA)k^4 + \omega^2 L^4 \{\alpha^2 \omega^4 + \rho A(EA - \gamma\omega^2)\}k^2 + \omega^4 L^6 \rho A^2 = 0. \tag{14}$$

Eq. (14) is the dispersion relation that gives the relation between wave number and frequency. At a specified frequency ω, Eq. (14) gives six values of wave number k, but they appear as $\pm$ pairs.

The relations between the coefficients A_i and B_i of Eq. (12) can be obtained by substituting Eq. (12) into Eq. (11a) as

$$B_i = (-1)^i \left\{ \frac{L^4 \rho A \omega^2 + L^2 \gamma \omega^2 k_i^2 + EIk_i^4}{Lk_i(L^2 \alpha \omega^2 + \beta k_i^2)} \right\} A_i = \lambda_i(\omega) A_i \quad (i = 1, 2, \ldots 6) \tag{15}$$

or simply

$$\{\mathbf{B}\} = [\text{diagonal}(\lambda_i)]\{\mathbf{A}\} \tag{16}$$

Substitute Eq. (16) into Eq. (12b) to express $\hat{U}$ as the function of A_i. The coefficients A_i can be determined by applying Eq. (12) into the boundary conditions of Eq. (8). The coefficients B_i can be then computed from Eq. (16). The coupling functions $\lambda_i(x)$ in Eq. (15) indicate the existence of the coupling between the axial-motion and the bending-motion of base beam. Infinite or zero values of $\lambda_i(x)$ simply imply the decoupling. When the piezoelectric layer thickness vanishes, it can be shown that the coefficients A_5, A_6, B_1, B_2, B_3, and B_4 indeed vanish to result in decoupled two problems: the pure bending-motion problem and the pure axial-motion problem.

The spectral nodal DOF defined in Fig. 2 can be expressed in terms of A_i, by using Eq. (12), as

$$\{\mathbf{x}\} = [\mathbf{Q}]\{\mathbf{A}\} \tag{17}$$

where $\mathbf{x}$ is the spectral nodal DOF vector defined by

$$\{\mathbf{x}\} = \{\hat{U}_1 \ \hat{W}_1 \ \hat{\Theta}_1 \ \hat{U}_2 \ \hat{W}_2 \ \hat{\Theta}_2\}^{\mathrm{T}} \tag{18}$$

Using Eqs. (16) and (17), the spectral displacement components of Eq. (12) can be represented in terms of the spectral nodal DOF vector as

$$\hat{W}(x) = [\mathbf{N}(x)][\mathbf{Q}]^{-1}\{\mathbf{x}\}$$

$$\hat{U}(x) = [\mathbf{N}(x)][\mathrm{diagonal}(\lambda_i)][\mathbf{Q}]^{-1}\{\mathbf{x}\}. \tag{19}$$

Substituting Eq. (12) into the spectral representations of the force-displacement relations of Eq. (9), the spectral components of the nodal forces and moments defined in Fig. 2 can be expressed in terms of A_i as

$$\{\mathbf{f}\} = [\mathbf{P}]\{\mathbf{A}\} \tag{20}$$

where

$$\{\mathbf{f}\} = \{\hat{N}_1 - \hat{N}^{\mathrm{e}} \quad \hat{Q}_1 \quad \hat{M}_1 + \hat{M}^{\mathrm{e}} \quad \hat{N}_2 + \hat{N}_2^{\mathrm{e}} \quad \hat{Q}_2 \quad \hat{M}_2 - \hat{M}^{\mathrm{e}}\}^{\mathrm{T}} \tag{21}$$

In Eq. (21), $\hat{N}_i$, $\hat{Q}_i$, $\hat{M}_i$ and are the nodal spectral components of axial force, the nodal transverse shear force and nodal bending moment defined in Fig. 2, respectively. Similarly, $\hat{N}^{\mathrm{e}}$ and $\hat{M}^{\mathrm{e}}$ are the nodal spectral components of piezoelectrically induced axial force and bending moment defined by

$$\hat{N}^{\mathrm{e}} = bd_{31}E_{\mathrm{p}}\hat{V}, \quad \hat{M}^{\mathrm{e}} = \frac{1}{2}hbd_{31}E_{\mathrm{p}}\hat{V}. \tag{22}$$

Eliminating the coefficients A_i from Eqs. (17) and (20) yields the spectral nodal force-nodal displacement relation as

$$\{\mathbf{f}\} = [\mathbf{P}][\mathbf{Q}]^{-1}\{\mathbf{x}\}] = [\mathbf{k}]\{\mathbf{x}\} \tag{23}$$

where $\mathbf{k}$ is the frequency-dependent spectral element matrix. Computer implementation to obtain $\mathbf{k}$ can be readily accomplished numerically. Explicit expression for $\mathbf{k}$ has become possible due to recent advance in symbolic computing (Fitch, 1985). Since the explicit expression for $\mathbf{k}$ is too lengthy, instead, the explicit expressions for $\mathbf{P}$ and $\mathbf{Q}$ are listed herein as

$$[\mathbf{P}] = \frac{1}{L^3}\begin{bmatrix} p_{11} & p_{11} & p_{12} & p_{12} & p_{13} & p_{13} \\ p_{21} & -p_{21} & p_{22} & -p_{22} & p_{23} & -p_{23} \\ p_{31} & p_{31} & p_{32} & p_{32} & p_{33} & p_{33} \\ -\mathrm{e}^{k_1}p_{11} & -\mathrm{e}^{-k_1}p_{11} & -\mathrm{e}^{k_2}p_{12} & -\mathrm{e}^{-k_2}p_{12} & -\mathrm{e}^{k_3}p_{13} & -\mathrm{e}^{-k_3}p_{13} \\ -\mathrm{e}^{k_1}p_{21} & -\mathrm{e}^{-k_1}p_{21} & -\mathrm{e}^{k_2}p_{22} & -\mathrm{e}^{-k_2}p_{22} & -\mathrm{e}^{k_3}p_{23} & -\mathrm{e}^{-k_3}p_{23} \\ -\mathrm{e}^{k_1}p_{31} & -\mathrm{e}^{-k_1}p_{31} & -\mathrm{e}^{k_2}p_{32} & -\mathrm{e}^{-k_2}p_{32} & -\mathrm{e}^{k_3}p_{33} & -\mathrm{e}^{-k_3}p_{33} \end{bmatrix}$$

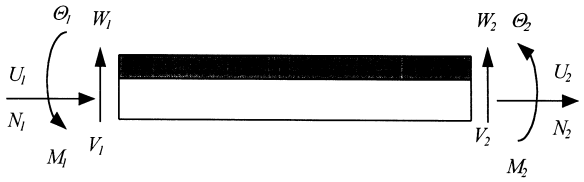

Fig. 2. Sign convention for the spectral element.

$$[\mathbf{Q}] = \begin{bmatrix} \lambda_1 & -\lambda_1 & \lambda_2 & -\lambda_2 & \lambda_3 & -\lambda_3 \\ 1 & 1 & 1 & 1 & 1 & 1 \\ k_1/L & -k_1/L & k_2/L & -k_2/L & k_3/L & -k_3/L \\ e^{k_1}\lambda_1 & -e^{-k_1}\lambda_1 & e^{k_2}\lambda_2 & -e^{-k_2}\lambda_2 & e^{k_3}\lambda_3 & -e^{-k_3}\lambda_3 \\ e^{k_1} & e^{-k_1} & e^{k_2} & e^{-k_2} & e^{k_3} & e^{-k_3} \\ (e^{k_1}k_1)/L & -(e^{-k_1}k_1)/L & (e^{k_2}k_2)/L & -(e^{-k_2}k_2)/L & (e^{k_3}k_3)/L & -(e^{-k_3}k_3)/L \end{bmatrix} \tag{24}$$

where

$$p_{1i} = k_i L(\beta k_i - EAL\lambda_i)$$

$$p_{2i} = L^2\omega^2\gamma k_i + EIk_i^3 - L^3\omega^2\alpha\lambda_i - L\beta k_i^2\lambda_i$$

$$p_{3i} = k_i L(L\beta\lambda_i - EIk_i) \tag{25}$$

The spectral elements can be assembled in a completely analogous way to that used for FEM. After applying the boundary conditions to the assembled result, the global system equation is reduced in the form as

$$[\mathbf{K}]\{\mathbf{X}\} = \{\mathbf{F}\} \tag{26}$$

where **K** is the global spectral matrix (or global dynamic stiffness matrix), **X** is the spectral DOF vector, and **F** is the spectral force vector. Eq. (26) can be solved for **X** and the results are applied into Eq. (19) to obtain the spectral displacement components. The inverse FFT algorithm is then used to obtain the time domain responses from the spectral displacement components.

4. Modal analysis

For modal analysis, the eigensolutions (i.e. natural frequencies and natural modes) should be obtained in prior. The eigensolutions can be obtained by the following steps.

1. Natural frequencies ω_n ($n = 1, 2, \ldots, \infty$) are computed numerically from the roots of the determinant of **K**, the global spectral matrix defined in Eq. (26).
2. At each natural frequency, six wave numbers $\pm k_i$ ($i = 1, 2, 3$) are computed from Eq. (14).
3. Coefficients A_i and B_i are then determined from Eq. (15) so as to satisfy boundary conditions.
4. Finally, the eigenfunctions (i.e. *exact* natural modes) are computed from Eq. (12) by using the wave numbers k_i and the coefficients A_i and B_i, all computed in the preceding steps.

By superposing the natural modes, the dynamic responses can now be obtained from

$$w(x, t) = \sum_n^\infty W_n(x)q_n(t)$$

$$u_b(x, t) = \sum_n^\infty U_n(x)q_n(t) \tag{27}$$

where W_n and U_n are the n-th natural modes of the bending motion and the axial motion, respectively, and $q_n(t)$ are the corresponding modal coordinates.

The orthogonality of normal modes is very useful for the modal analysis. Thus, the orthogonality property for the present axial-bending coupled problem will be derived in the following.

Since the eigensolutions are the general solutions of Eq. (11), the n-th eigensolutions should satisfy the following two equations:

$$EIW_n'''' - \omega_n^2 \rho A W_n = \omega_n^2(-\gamma W_n'' + \alpha U_n') + \beta U_n''''$$

$$EAU_n'' + \omega_n^2 \rho A U_n = \omega_n^2 \alpha W_n' + \beta W_n'''. \tag{28}$$

By using Eq. (9) (with zero applied voltage), Eq. (28) can be rewritten as

$$\omega_n^2(\rho A W_n + \alpha U_n') = M_n'' + \omega_n^2 \gamma W_n'' \tag{29a}$$

$$\omega_n^2(\rho A U_n - \alpha W_n') = -N_n' \tag{29b}$$

where N_n and M_n represent the resultant axial force and bending moment, respectively, at the n-th natural mode.

Multiply Eq. (29a) by W_m and Eq. (29b) by U_m, integrate the results from $x = 0$ to $x = L$, and finally sum two integrations to obtain

$$\omega_n^2 \int_0^L (\rho A U_n U_m + \rho A W_n W_m + \alpha U_n' W_m - \alpha W_n' U_m)\, \mathrm{d}x = -\int_0^L N_n' U_m \, \mathrm{d}x + \int_0^L M_n'' W_m \, \mathrm{d}x + \omega_n^2 \int_0^L \gamma W_n'' W_m \, \mathrm{d}x. \tag{30}$$

Similarly, for the m-th eigensolutions, one may obtain

$$\omega_m^2 \int_0^L (\rho A U_n U_m + \rho A W_n W_m + \alpha U_m' W_n - \alpha W_m' U_n)\, \mathrm{d}x = -\int_0^L N_m' U_n \, \mathrm{d}x + \int_0^L M_m'' W_n \, \mathrm{d}x + \omega_m^2 \int_0^L \gamma W_m'' W_n \, \mathrm{d}x. \tag{31}$$

Subtracting Eq. (30) from Eq. (31), integrating by parts, applying the boundary conditions, and accomplishing a further manipulation may yield the orthogonality property as

$$\int_0^L \{\rho A(U_n U_m + W_n W_m) - \alpha(U_n W_m' + U_m W_n') + \gamma W_n' W_m'\}\, \mathrm{d}x = m_n \delta_{mn} \tag{32}$$

where m_n is the modal mass and it is computed from

$$m_n = \int_0^L \{\rho A(U_n^2 + W_n^2) - \alpha(U_n W_n' + U_n W_n') + \gamma W_n'^2\}\, \mathrm{d}x. \tag{33}$$

Once the orthogonality property of Eq. (32) is derived, the forced vibration responses of the present axial-bending coupled problem can be readily obtained by using the modal analysis method.

The equations of motion for the forced vibration are given by

$$EIw'''' + \rho A \ddot{w} + \alpha \ddot{u}_b' - \beta u_b''' - \gamma \ddot{w}'' = p(x, t)$$

$$EAu_b'' - \rho A\ddot{u}_b + \alpha\ddot{w}' - \beta w'''' = -\tau(x, t) \tag{34}$$

where $p(x, t)$ and $\tau(x, t)$ represent the external forces acting along the beam transversely and longitudinally, respectively. Substituting Eq. (27) into Eq. (34) and applying the orthogonality property of Eq. (32), decoupled modal equations can be derived as

$$\ddot{q}_n(t) + \omega_n^2 q_n(t) = \frac{f_n}{m_n} \tag{35}$$

where f_n is the nodal force defined by

$$f_n = \int_0^L \{\tau(x, t)U_n + p(x, t)W_n\}\, dx. \tag{36}$$

5. Numerical examples

The validity and accuracy of the spectral element and the modal analysis approach introduced for the axial-bending coupled elastic-piezoelectric two-layer beam problems are verified in this section by comparing with the solutions obtained by finite element analysis and experiment. For the finite element analysis, a finite element model is also formulated from the present axial-bending coupled equations of motion by using the same kinematics (e.g. nodal displacements and shape functions) and formulation procedure as introduced by Liao (1997).

As illustrative examples, two cantilevered laminate beams are considered. The base beams used for both laminate beams are identical in geometry and material: length $L = 0.2616$ m, thickness $h_b = 0.00286$ m, Young's modulus $E_b = 71$ GPa, and mass density $\rho_b = 2700$ kg/m^3. The base beam of the first laminate beam is *fully* covered, from the fixed root to the free end, with a piezoelectric constraining layer. On the other hand, the base beam of the second laminate beam is *partially* covered with a piezoelectric patch of length 0.1016 m, starting at 0.027 m distance from the fixed root. The widths of the base beam, the piezoelectric layer, and the patch are all 0.0127 m. The piezoelectric layer or patch has Young's modulus $E_p = 64.9$ GPa, elastic stiffness $C_{11}^D = 74$ GPa, piezoelectric constant $d_{31} = -175 \times 10^{-12}$ m/V, and mass density $\rho_p = 7600$ kg/m^3.

Tables 1 and 2 compare the natural frequencies obtained by SEM and FEM for the *fully* covered

Table 1
The natural frequencies obtained by SEM and FEM for the *fully* covered beam (n = total number of finite elements or spectral elements)

Modes	ω_{SEM} (Hz)	ω_{FEM} (Hz)				
	$n = 1$	$n = 10$	$n = 20$	$n = 50$	$n = 100$	$n = 150$
1st	30.04	30.05	30.04	30.04	30.04	30.04
2nd	188.22	188.58	188.31	188.23	188.22	188.22
3rd	526.89	529.40	527.50	526.99	526.91	526.90
4th	1032.13	1041.56	1034.36	1032.48	1032.22	1032.17
5th	1705.41	1731.48	1711.36	1706.34	1705.65	1705.52
10th	6067.52	6463.04	6143.95	6078.60	6070.25	6068.73
15th	13063.72	15609.61	13449.38	13114.36	13075.96	13069.13
20th	22622.09	29135.45	23911.50	22774.05	22657.92	22637.84

Table 2
The natural frequencies obtained by SEM and FEM for the *partially* covered beam (n = total number of finite elements or spectral elements)

Modes	ω_{SEM} (Hz)	ω_{FEM} (Hz)				
	$n = 3$	$n = 10$	$n = 20$	$n = 50$	$n = 100$	$n = 150$
1st	32.94	32.95	32.95	32.94	32.94	32.94
2nd	165.32	165.41	165.34	165.32	165.32	165.32
3rd	482.43	483.09	482.58	482.46	482.44	482.44
4th	938.39	940.90	938.90	938.47	938.41	938.40
5th	1604.40	1612.86	1605.95	1604.62	1604.45	1604.42
10th	5797.62	5972.64	5826.75	5800.89	5798.38	5797.95
15th	12579.64	14790.15	12760.97	12596.13	12583.24	12581.20
20th	22421.84	30892.99	22620.96	22445.59	22427.65	22424.41

beam and the *partially* covered beam, respectively. In both tables, n indicates the total number of finite elements or spectral elements used in the analysis. For spectral element analysis, the possible minimum number of spectral elements is one for the *fully* covered beam and three for the *partially* covered beam, as indicated in the tables. Both tables show that, as the total number of finite elements used in FEM is increased, the natural frequencies by FEM gradually converge to the natural frequencies by SEM at all natural frequencies. This may prove that SEM provides very accurate solutions with using only minimum number of spectral elements. The validity and accuracy of the modal analysis method (MAM) introduced in this paper is also verified in Figs. 3 and 4. Fig. 3 shows the percent receptance error for the axial motion of base beam and Fig. 4 for the bending motion, both for the *fully* covered beam. To excite the cantilevered beam, as indicated in the figures, a point load is applied at the free end without applying voltage. As expected, the receptance (the frequency response function defined by displacement/force) obtained by MAM indeed gradually converges to that obtained by SEM as the total number of normal modes considered in modal analysis is increased. The percent receptance errors for the axial motion and bending motion show that the bending motion can be predicted more accurately at a specified total number of normal modes considered in modal analysis. Thus, in the present axial-bending

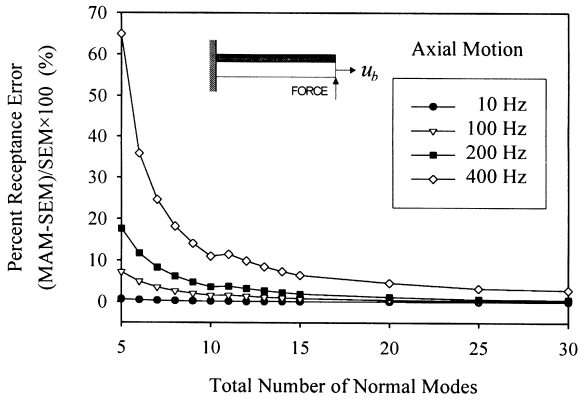

Fig. 3. Percent receptance error for the axial motion vs the total number of normal modes used in the modal analysis: SEM and MAM represent the receptances obtained by spectral element method and modal analysis method, respectively.

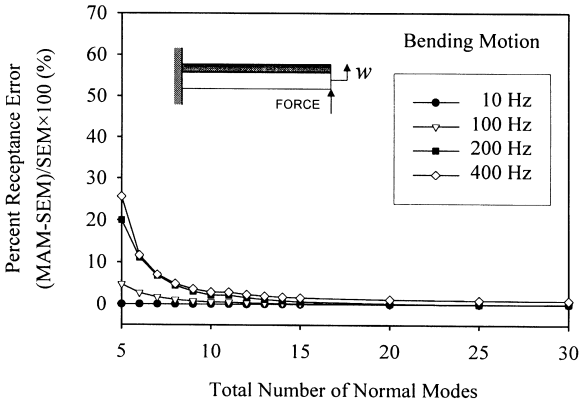

Fig. 4. Percent receptance error for the bending motion vs the total number of normal modes used in the modal analysis: SEM and MAM represent the receptances obtained by spectral element method and modal analysis method, respectively.

coupled problem, more normal modes summation is required for the axial motion to meet the specified solution accuracy.

Fig. 5 compares the receptances of bending motion obtained by SEM, FEM, and experiment. The experimental data is cited from the work by Liao (1997). The natural frequencies predicted by SEM and FEM are so close to each other within the frequency range of experiment by Liao (1997) that the difference is not apparent in Fig. 5. However, as can be confirmed from Table 2, the natural frequencies predicted by FEM are always larger than those by SEM. This fact may conclude that SEM provides more reliable dynamic characteristics of an elastic-piezoelectric two-layer beam than FEM.

Finally, the effects of thickness ratio ($r = h_a/h_b$) on the natural frequencies of the cantilevered laminate beams are illustrated in Figs. 6 and 7 for the *partially* covered beam and for the *fully* covered beam, respectively. Both figures clearly show that every natural frequency is getting smaller toward the corresponding natural frequency of the base beam layer as the thickness ratio decreases. From Eq. (5), it can be shown that the bending motion of the base beam layer should be completely decoupled from the axial motion when the piezoelectric layer (or patch) thickness vanishes completely. Figs. 6 and 7 show

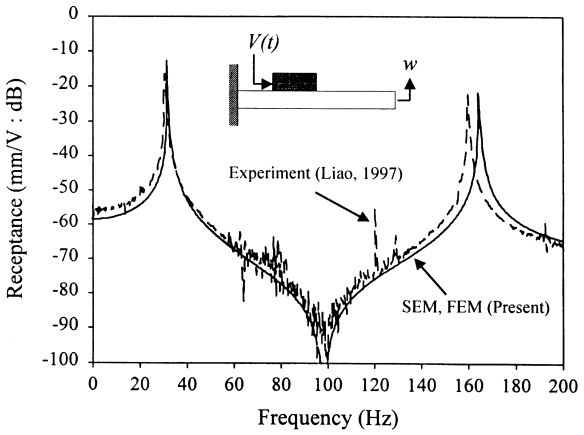

Fig. 5. Comparison of the receptances of bending motion obtained by SEM, FEM, and experiment (Liao, 1997).

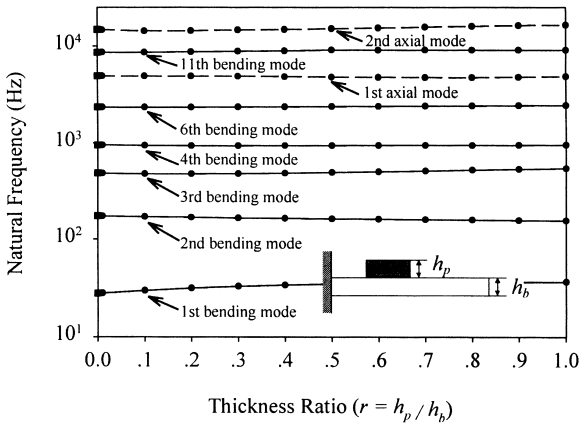

Fig. 6. Thickness ratio dependence of the natural frequencies of the *partially* covered beam.

that the natural frequencies at zero thickness ratio (marked by the square dots) are indeed identical to the natural frequencies for the pure axial motion and pure bending motion of the base beam layer.

6. Concluding remarks

Accurate prediction of the dynamic characteristics of a piezoelectrically actuated beam is very important for successful vibration or noise controls. It has been well recognized that spectral elements provide very accurate solutions for such simple structures as beams. Thus, this paper introduces a spectral element method (SEM) and a spectral-element based modal analysis method (MAM) for elastic-piezoelectric two-layer beams.

First, the axial-bending coupled equations of motion are derived for the elastic-piezoelectric two-layer beam by using Hamilton's principle. The spectral element is then formulated by using the exact eigenfunctions spectrally formulated from the coupled governing equations of motion. The modal

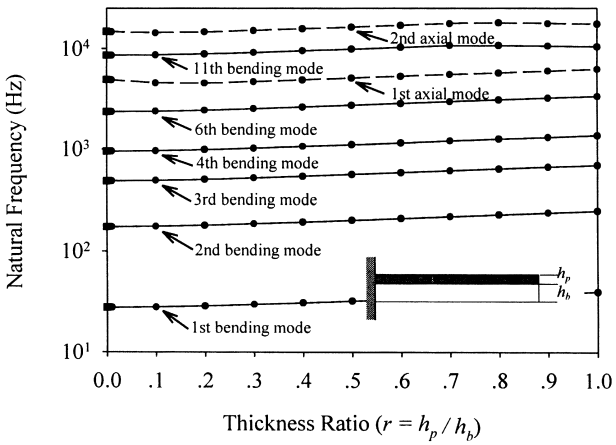

Fig. 7. Thickness ratio dependence of the natural frequencies of the *fully* covered beam.

analysis approach for the present axial-bending coupled problem is also introduced by deriving the orthogonality property of the exact eigenfunctions.

The validity and the accuracy of SEM and MAM introduced herein are verified through some illustrative examples. It is shown that the dynamic characteristics predicted by FEM and MAM generally converge to the dynamic characteristics by SEM as the number of finite elements and normal modes, respectively, is increased. Thus, due to the high accuracy of the spectral element formulated in this paper, SEM may provide very reliable dynamic characteristics of the elastic-piezoelectric two-layer beams.

Acknowledgements

This study is supported by the 1999 Inha University Research Fund.

References

Bai, J.M., Sun, C.T., 1993. A refined theory of flexural vibration for viscoelastic damped sandwich beams. In: Proceeding of Damping '93, San Francisco, CA, 3, pp. 319–329.

Banerjee, J.R., 1989. Coupled bending-torsional dynamic stiffness matrix for beam elements. International Journal for Numerical Methods in Engineering 28, 1283–1298.

Banerjee, J.R., 1997. Dynamic stiffness formulation for structural elements: a general approach. Computers and Structures 63 (1), 101–103.

Banerjee, J.R., Guo, S., Howson, W.P., 1996. Exact dynamic stiffness matrix of a bending-torsion coupled beam including warping. Computers and Structures 59 (4), 613–621.

Baz, A., 1993. Active constrained layer damping. In: Proceeding of Damping '93, San Francisco, CA, 3, pp. 187–209.

Bishop, R.E.D., Cannon, S.M., Miao, S., 1989. On coupled bending and torsional vibration of uniform beams. Journal of Sound and Vibration 131 (3), 457–464.

Crawley, E.F., de Luis, J., 1987. Use of piezoelectric actuators as elements of intelligent structures. AIAA Journal 25 (10), 1373–1385.

Dokumaci, E., 1987. An exact solution for coupled bending and torsion vibrations of uniform beams having single cross-sectional symmetry. Journal of Sound and Vibration 119 (3), 443–449.

Doyle, J.F., 1988. A spectrally formulated finite element for longitudinal wave propagation. International Journal of Analytical and Experimental Modal Analysis 3, 1–5.

Fitch, J., 1985. Solving algebraic problems with REDUCE. Journal of Symbolic Computation 1, 211–227.

Hess, M.S., 1969. The end problem for a laminated elastic strip—I. The general solution. Journal of Composite Materials 3, 262–280.

Kerwin Jr, E.D., 1959. Damping of flexural waves by a constrained viscoelastic layer. Journal of the Acoustical Society of America 31 (7), 952–962.

Lee, U., Lee, J. 1997. Dynamic analysis of one- and two-dimensional structures using spectral element methods. In: Proceedings of the Sixth International Conference on Recent Advances in Structural Dynamics. ISVR, University of Southampton, pp. 263–277.

Lesieutre, G.A., Lee, U., 1996. A finite element for beams having segmented active constrained layers with frequency-dependent viscoelastics. Smart Structures and Materials 5, 615–627.

Leung, A.Y.T., 1993. Dynamic Stiffness and Substructures. Springer-Verlag, London.

Leung, A.Y.T., Zhou, W.E., 1996. Dynamic stiffness analysis of laminated composite plates. Thin-Walled Structures 25 (2), 109–133.

Liao, W.H., 1997. Active-passive hybrid structural control: an enhanced active constrained layer damping treatment with edge elements. Ph.D. Thesis, The Pennsylvania State University, PA.

Mead, D.J., Markus, S., 1969. The forced vibration of a three-layer, damped sandwich beam with arbitrary boundary conditions. Journal of Sound and Vibration 10 (2), 163–175.

Mead, D.J., 1982. A comparison of some equations for the flexural vibration of damped sandwich beams. Journal of Sound and Vibration 83 (3), 363–377.

Nayfeh, S.A., Slocum, A.H. 1997. Flexural vibration of a viscoelastic sandwich beam in its plane of lamination. In: Proceedings of the 1997 ASME Design Engineering Technical Conferences, Sacramento, CA.

Oberst, H., 1952. Uber Die Dampfung Der Biegeschwinggungen Dunner Bleche Durch Fest Haftende Belage. Acusta 2, 181–194.

Rao, Y.V.K.S., Nakra, B.C., 1974. Vibrations of unsymmetrical sandwich beams and plates with viscoelastic cores. Journal of Sound and Vibration 34 (3), 309–326.

Robbins, D.H., Reddy, J.N., 1991. Analysis of piezoelectrically actuated beams using a layer-wise displacement theory. Computers and Structures 41 (2), 265–279.

Shi, G., Atluri, S.N., 1990. Active control of nonlinear dynamic response of space-frames using piezo-electric actuators. Computers and Structures 34 (4), 549–564.

Yan, M.J., Dowell, E.H., 1972. Governing equations for vibrating constrained-layer damping sandwich plates and beams. Journal of Applied Mechanics 39, 1041–1046.